Energetics of Organic Solid-State Reactions: The Topochemical Principle and the Mechanism of the Oligomerization of the 2,5-Distyrylpyrazine Molecular Crystal

N. M. Peachey and C. J. Eckhardt*

Contribution from the Department of Chemistry, University of Nebraska-Lincoln, Lincoln, Nebraska 68588-0304

Received November 30, 1992

Abstract: The 30-fold difference in reactivity of the isomorphous crystals of 2,5-distyrylpyrazine (DSP) and 1,4-bis-(3-pyridyl-2-vinyl)benzene (P2VB), two isoelectronic and nearly structurally identical molecules, has remained an important problem in organic solid-state chemistry. This disparity of oligomerization rates in the solid state is further accentuated by the fact they have similar rates of reaction in solution. The differences in reactivity of these molecular crystals cannot be explained from topochemical considerations. To more completely understand the discrepancy of reactivity of these archetypical photochemical solid-state reactions, the oligomerization of DSP has been reexamined. The polarized, low-temperature reflection spectra were obtained for the DSP monomer crystal and two excited states are found to be involved in the oligomerization. These two states have exciton branches in the same frequency region. The most prominent is a $\pi^* \leftarrow \pi$ transition which forms a delocalized exciton. The second, less evident one, is an $\pi^* \leftarrow$ n transition which is shown to be a localized exciton that couples with the lattice phonons. This exciton–phonon coupling generates a lattice distortion which provides a trap for the delocalized exciton to initiate the photoreaction. The exciton trapping observed in DSP is not available to P2VB. This mechanism demonstrates the importance of considering the collective nature of solid-state properties in the investigation of organic solid-state reactions and resolves a long-standing question in organic solid-state chemistry.

I. Introduction

Reactions in the organic solid state have attracted considerable attention since the detailed investigation of cinnamic acids by G. M. J. Schmidt and co-workers.[1] This interest arises from a variety of unique features of the crystalline phase. The solid state provides geometric control, unavailable in other phases, that dictates both the course of reaction as well as the structure of its products.[2] Unlike reactions in the fluid phases, there are seldom secondary reactions. Furthermore, the products obtained from a solid-state reaction may not be the same as those of the reaction in other phases. For example, a solid-state reaction can be the only method of synthesizing some single crystal polymers.

Distinctive to the solid phase is the collective nature of its physical properties due to the ordered aggregation of molecules. These collective properties can effect global, macroscopic transformations resulting from local, microscopic perturbations. This is particularly evident in phase transitions and chemical reactions.[3] An additional consequence of the solid state is the structural rigidity forcing the constituent molecules to remain fixed in space. The unique relation of structure to reactivity has led to labeling those reactions as "topochemical" wherein the structure of the products is dictated by the geometry and proximity of the reactive sites of the precursors in the lattice.[4] Because of this dependence upon geometry, investigations of these solid-state reactions have followed the lead of Schmidt and focused predominantly on structural studies to rationalize the reaction pathways. The great success of this approach has, however, led to neglect of other important facets of these mechanisms. This is regrettable since other factors can significantly affect the course of a solid-state reaction. On a more basic level, structure is a consequence of energetics, and, thus, investigation of the latter is needed and appropriate.

The topochemical postulate implies that there should always be a direct relationship between geometry and reactivity. But there are numerous examples where this does not obtain. One of the clearest cases is the difference in reactivity of oligomerization between the 2,5-distyrylpyrazine (DSP) and the 1,4-bis(3-pryidyl-2-vinyl)benzene (P2VB) molecular crystals. The reactive double

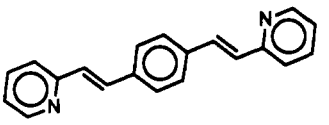

P2VB

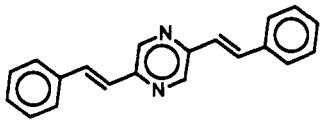

DSP

bonds of DSP are 3.939 Å apart[5] while in the isomorphic P2VB crystal, they are separated by only 3.910 Å.[6] A summary of their crystallographic parameters is given in Table I and their packing is shown in Figure 1. According to topochemical considerations, the P2VB crystal should be significantly more reactive than DSP, but the reverse is true. In the crystal, DSP is about 30 times more reactive than P2VB, while in solution, the two molecules have comparable rates of reaction.[3] The failure of the topochemical principle to predict the relative reactivities of these

(1) Schmidt, G. M. J., In *Solid State Chemistry*; Ginsburg, D. Ed.; Verlag Chemie: Weinheim, Germany, 1976; p 2.
(2) Kearsley, S. K. In *Organic Solid State Chemistry*; Desiraju, G. R., Ed.; Elsevier: New York, 1987; p 69.
(3) Nagaosa, N.; Ogawa, T. *Phys. Rev. B* **1989**, *39*, 4472.
(4) Wegner, G. *Pure Appl. Chem.* **1977**, *49*, 443.
(5) Sasada, Y.; Shimanouchi, H.; Nakanishi, H.; Hasegawa, M. *Bull. Chem. Soc. Jpn.* **1971**, *44*, 1262.
(6) Nakanishi, H.; Ueno, K.; Hasegawa, M. *Chem. Lett.* **1972**, 301.

0002-7863/93/1515-3519$04.00/0

Table I. Crystallographic Data for DSP and P2VB

	a, Å	b, Å	c, Å	space group	Z
DSP	20.639	9.599	7.655	*Pbca*	4
P2VB	21.060	9.567	7.311	*Pbca*	4

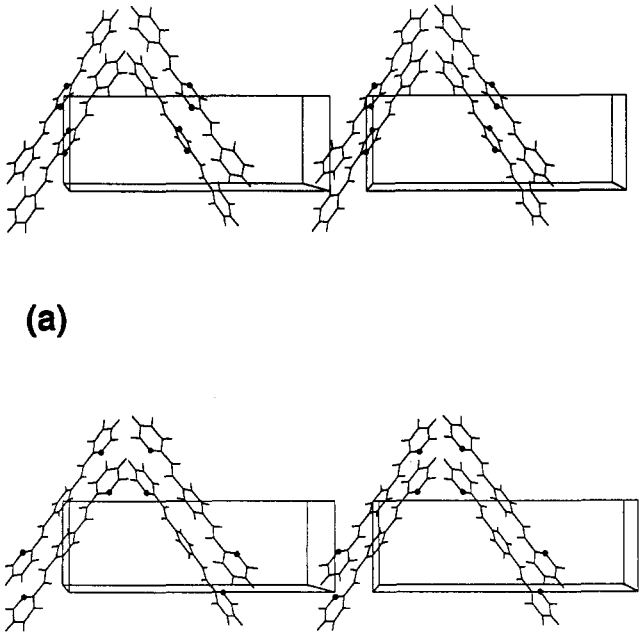

Figure 1. The stereoplots viewed along the [010] direction of (a) DSP and (b) P2VB. In each case the black dots indicate the positions of the nitrogen atoms.

two molecular crystals invites investigation of the energetic and dynamic processes.

To better understand solid-state reactions, a more comprehensive approach is required which combines structural considerations with photophysics and lattice dynamics. Since most of these reactions are photochemical, the involved excited states must first be well-defined. In the solid state, the electronic excitation becomes complicated by collective interactions such as excitons and phonons. These collective excitations can migrate through the lattice and form defects and traps. Another photoeffect which can influence the reaction is the formation of excimers. These dimers which form upon excitation can severely distort the molecules in the lattice and become initiation sites for the reaction. Such effects have been proposed to influence the differing rates of reaction in DSP and P2VB.[7] A third consequence of the crystalline order is the ability to couple an electronic excitation with a lattice vibration.[8] Such exciton–phonon coupling can create a lattice distortion which can trap energy to initiate product formation. This mechanism has been proposed to explain the reactivity of DSP and P2VB.[9] Clearly, the potential roles of excitons, excimers, and exciton–phonon interactions require that reactive crystals be examined to establish the role of these phenomena in their photochemical transformation. These investigations, combined with structural studies, can provide a much clearer understanding of these reactions.

The archetypical organic crystal-to-crystal reactions of DSP and P2VB were first studied by Hasegawa and co-workers.[10]

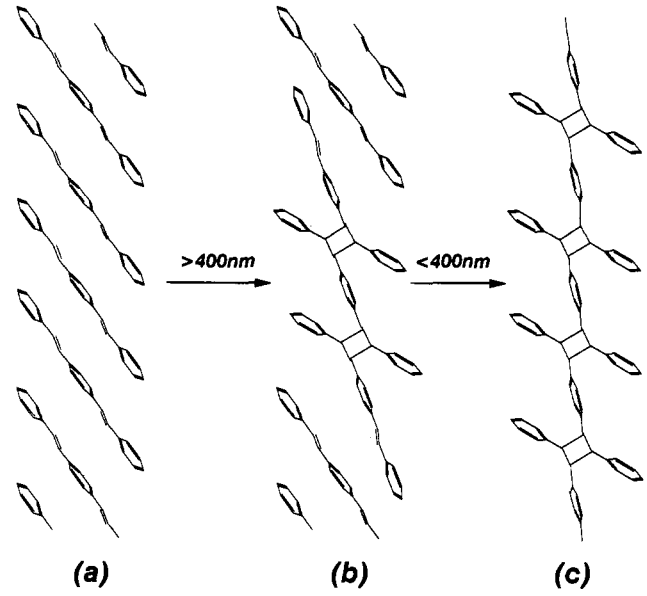

Figure 2. The photopolymerization reaction of DSP: (a) monomer (b) oligomer, and (c) polymer.

They found that the DSP molecular crystal undergoes a photochemical reaction when irradiated with light of shorter wavelength than about 450 nm. Further investigation revealed that this is, in fact, a two stage reaction which produces oligomers of approximately three to five monomer units if illuminated with light in the range of 400–450 nm.[11] When the oligomer crystals are irradiated with light of wavelength shorter than 400 nm, a high polymer results. However, illumination of the monomer crystal at wavelengths shorter than 400 nm leads directly to the high polymer. These results are shown schematically in Figure 2.

Although the oligomer and polymer products were highly crystalline, Hasegawa et al. found that the original monomer crystals retained their original shape only at low conversion. Upon irradiation, the crystals cracked and yielded product fibers. The discovery of the DSP photopolymerization has prompted a variety of studies which have attempted to account for its observed duality of reaction products as well as its high degree of reactivity.[7,12–14]

Any comprehensive description of solid-state reactions must account for problems such as the discrepancy between the reactivities of DSP and P2VB. Since these molecules have quite similar molecular and crystallographic structures as well as similar reactivities in solution, the contrast found in the solid state must be due to properties unique to that phase. Furthermore, aspects other than crystallographic features must be investigated to explain this great difference in solid-state reactivity which violates the topochemical principle. This requires that the rationale necessary to account for this apparent discrepancy must be sought from energetic and dynamic processes within the lattice. To achieve this, the low-temperature, polarized reflection spectra were obtained from single crystals of monomer DSP. The low-temperature reflection spectra allow the investigation of the $\pi^* \leftarrow \pi$ transition which has been thought to be responsible for the photoreaction[10] as well as any additional transitions which happen to be in this energy region.

After reviewing the experimental procedures, section II of this paper will discuss the effect of impurities in DSP. This section

(7) Ebied, E.-Z.; Bridge, N. J. *J. Chem. Soc., Faraday Trans. 1* **1984**, *80*, 1113.
(8) Hochstrasser, R. M.; Prasad, P. N. *J. Chem. Phys.* **1971**, *56*, 2814.
(9) Prasad, P. N. In *Crystallographically Ordered Polymers*; ACS Symposium Series 337, Sandman, D. J., Ed.; American Chemical Society: Washington, DC, 1986; p 106.
(10) Hasegawa, M.; Suzuki, Y.; Suzuki, F.; Nakanishi, H. *J. Polym. Sci. A-1* **1969**, *7*, 743. Nakanishi, H.; Suzuki, Y.; Suzuki, F.; Hasegawa, M. *J. Poly. Sci. A-1* **1969**, *7*, 753.
(11) Tamaki, T.; Suzuki, Y.; Hasegawa, M. *Bull. Chem. Soc. Jpn.* **1972**, *45*, 1988.
(12) Hasegawa, M. *Adv. Polym. Sci.* **1982**, *42*, 1.
(13) Peachey, N. M.; Eckhardt, C. J. *Chem. Phys. Lett.* **1992**, *188*, 462.
(14) Braun, H.-G.; Wegner, G. *Makromol. Chem.* **1983**, *184*, 1103.

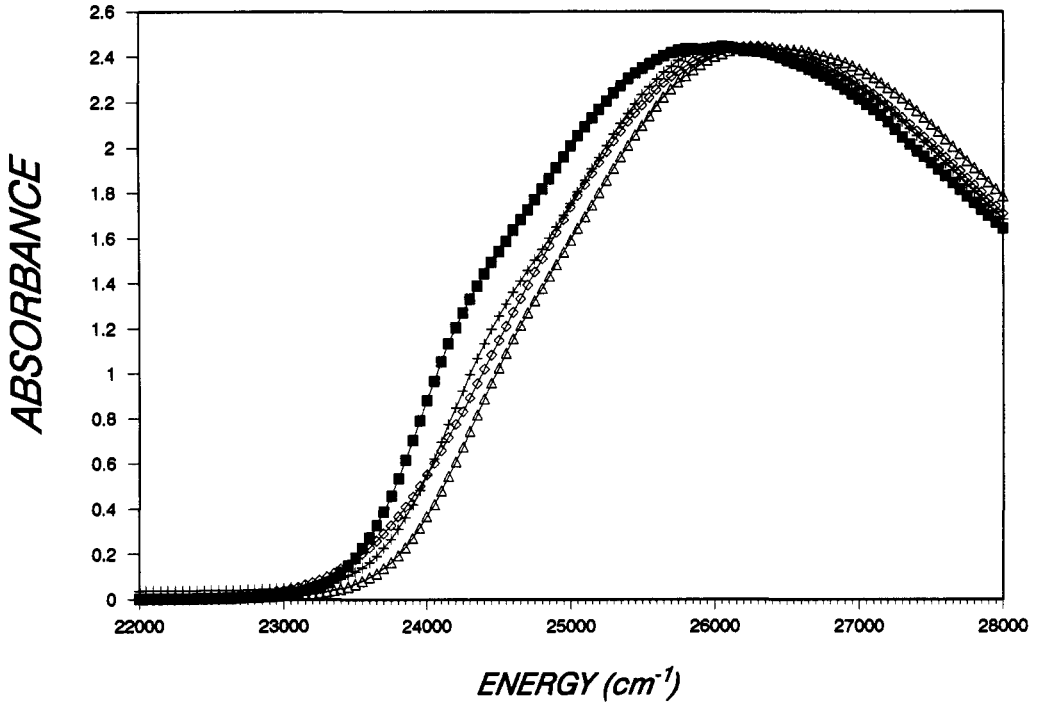

Figure 3. Solution spectra of DSP in benzene (■), in methanol (◇), in tetrahydrofuran (+), and in acetonitrile (Δ).

concludes with a discussion of the theoretical models used to obtain calculational results for the electronic structure and excitonic interactions. Section III begins with the analysis of the electronic structure of DSP. Following this, the Davydov splitting observed between different factor group symmetry components of the excitation in the crystal spectrum are investigated to elucidate the excitonic behavior of this crystal. Calculations are then presented to establish the character of these excitons. Next, the exciton–phonon interactions in the DSP molecular crystal are examined. This section concludes with a formulation of a mechanism for the solid-state reactivity of DSP using the experimental and calculational results.

II. Procedures and Results

A. Experimental. DSP was synthesized according to the procedure described by Hasegawa.[8] Initially, the product was purified by recrystallization and three successive sublimations. This was found to be inadequate to remove all impurities, so the recrystallized material was purified by column chromatography using reagent grade benzene (Fischer Scientific) as the eluent. The column was packed with silica gel 60, 230–400 mesh (E. M. Science). Purification by zone refining proved unproductive since DSP decomposes on repetitive melting as noted elsewhere.[6] Pale yellow crystals of the orthorhombic α-form were grown by slow evaporation from a saturated solution of DSP in tetrahydrofuran in the dark. Solution spectra in reagent grade benzene, methanol, tetrahydrofuran, and acetonitrile were obtained at ambient temperature on Model 8452A Hewlett-Packard and Cary Model 14 spectrophotometers. As shown in Figure 3, the lower energy shoulder of the DSP spectrum is blue-shifted in polar solvents. The electronic transition dipole strength for this band is 2.86 Å^2. This transition displays a vibronic progression of 1000 cm^{-1} which corresponds to an active mode observed in the molecular Raman spectrum. The Franck–Condon factors obtained from deconvolution of the solution spectrum are ξ^2 = 0.19, 0.31, 0.23, 0.17, and 0.10.

The low-temperature, polarized, single crystal specular reflection spectra of DSP were obtained at 12 K from the (100) and (010) faces of the crystal. Although the region of interest for the photochemistry is from 20 000 to 30 000 cm^{-1}, the spectra from 12 000 to 44 400 cm^{-1} were obtained for light polarized along each of the crystal axes. A single channel microspectroreflectometer utilizing a THR 1500 monochromator (Jobin Yvon) and a 1000 W Xe arc lamp (Oriel) was used. The crystal was cooled using a Model 21 refrigerator (CTI-Cryogenics). The reflection data for each principal direction were corrected to absolute reflectivity and subsequently transformed to absorption spectra using a Fourier transform[15] (Figure 4).

B. Impurities. A photochemical reaction can be significantly altered by the existence of impurities. This is particularly true in solid-state reactions where the excitations can migrate through the lattice and be readily trapped by contaminants. Traps can either be quenchers causing the excitation energy to dissipate rather than initiate a photochemical reaction or be reaction initiators in which case they become defect sites from which the product grows. In either case, these defects in the lattice can cause the reaction to proceed along a much different pathway than would be observed in a perfect crystal. Impurity traps were suspected to have a role in DSP by noting that the reaction can be initiated by prolonged irradiation at 490 nm although this is at much lower energy than is required to form the first excited state of DSP. When these crystals were irradiated,[16] they were observed initially to emit a yellowish green hue. Upon additional irradiation, the observed emission became blue. This suggested that impurities were responsible for the initial emission. As the reaction proceeds, the excitation becomes less mobile due to formation of polymer thereby reducing the probability that it will encounter impurity sites. Previous work has also implicated the presence of such traps in DSP.[6]

In order to test for the presence of impurities, a sample of DSP was chromatographed. Crystals grown from this highly purified material required slightly shorter wavelength illumination than the less purified crystals to initiate the reaction and the previously reported yellowish green emission was absent. Furthermore, upon irradiation these crystals were not nearly as prone to cracking as the less pure ones and complete conversion to oligomer can be achieved without disintegration. Fully oligomerized crystals are completely colorless with some cracks observed through the bulk.

(15) Peterson, C. W.; Knight, B. W. *J. Opt. Soc. Am.* **1973**, *63*, 1238.
(16) Details of irradiation to form pure oligomer crystals to be published elsewhere.

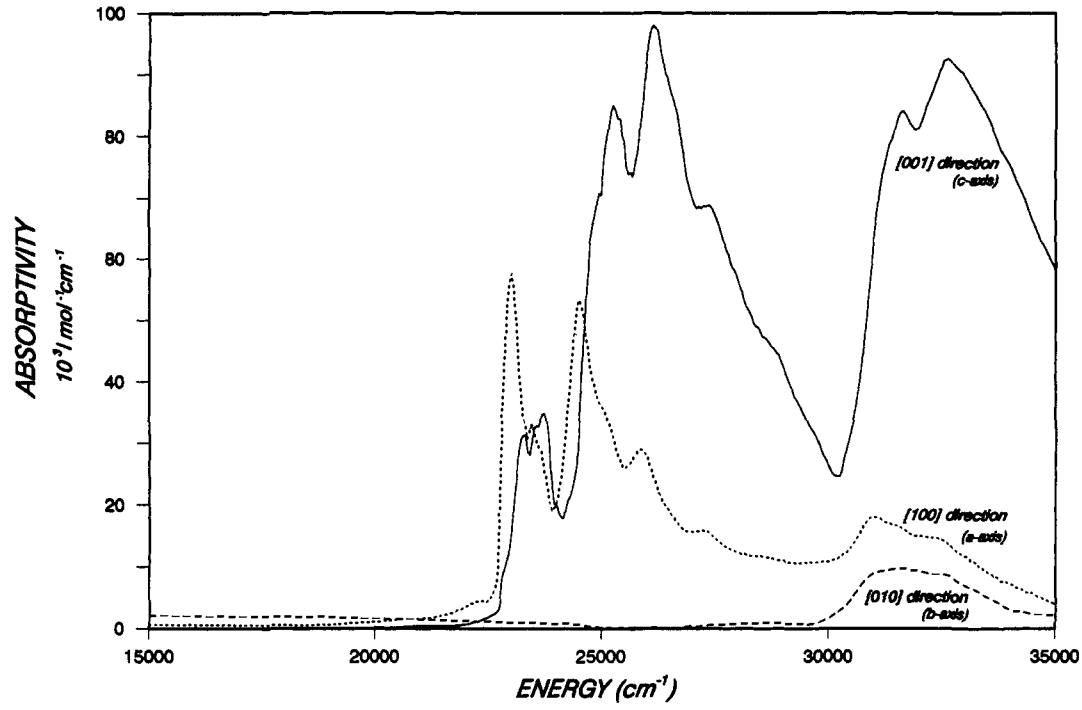

Figure 4. The polarized, low-temperature absorption spectra of the DSP monomer along the [100] direction (···), the [010] direction (- -), and the [001] direction (—). The structure below 23 000 cm^{-1} is an artifact of the transform.

These observations demonstrate the existence of impurity traps even in recrystallized and sublimed DSP and underscore the importance of extensive and proper purification of photoreactive crystals. Indeed, since DSP does not sublime readily, the heating required to vaporize the monomer molecules reintroduces impurities. Thus DSP monomer, which has been purified by column chromatography, is recontaminated by subsequent vacuum sublimation.

Previous studies of this reaction have used only recrystallization or have combined other purification methods with vacuum sublimation. Thus, the role of impurities is an important but ill-defined complication of reported results in the literature. Since the presence, nature, and concentration of impurities are expected to significantly alter the photochemical process, some of the disagreement between previous reports over the mechanism and products of the DSP reaction may arise from these contaminants.

C. Calculational Approaches. To aid in the analysis of the DSP spectrum, an INDO/S calculation was performed for the monomer molecule. This calculation was based on the approach of Ridley and Zerner[17] who used an LCAO-MO-SCF-CI model specifically designed to accommodate $\pi^* \leftarrow$ n transitions such as those encountered in nitrogen heterocycles. This was necessary since many of the calculational methods which reproduce $\pi^* \leftarrow \pi$ spectra reasonably well are not as successful when calculating $\pi^* \leftarrow$ n transitions. The calculation is carried out in two steps. First the ground state is calculated to acquire molecular orbital coefficients and eigenvalues. This is followed by configuration interaction (CI). To determine the orbitals necessary for the CI calculation, the number included was increased until no significant improvement was observed in the calculational results by further addition of orbitals. For the DSP calculation, 16 filled and 16 unfilled orbitals were used.

The exciton calculations were carried out by consideration of single-exciton states only. Since in most molecular crystals the energy gap between the ground and excited states is large, the theory assumes no mixing between these states. The Hamiltonian for exciton interactions is[18,19]

$$\mathcal{H}_{ex} = E_G + \sum_{s,u}(\Delta\epsilon_s + D_s)B^\dagger_{su}B_{su} + \frac{1}{2}\sum_{s,u}\sum_{s',u'}\langle\varphi^o_s\varphi^{u'}_{s'}|V_{ss'}|\varphi^u_s\varphi^o_{s'}\rangle(B_{su} + B^\dagger_{su})(B_{s'u'} + B^\dagger_{s'u'}) \quad (1)$$

where E_G is the ground-state energy for the free molecule, $B^\dagger$ and B are the creation and annihilation operators for excitons, and $\Delta\epsilon_s$ is the excitation energy. $D_s = \sum_{s\neq u} D_{su}$ where D_{su} is the van der Waals interaction between molecules s and u upon electronic excitation of molecule s. The potential energy operator $V_{ss'}$ relates the interaction between a molecule in state s and s'. The exciton interaction Hamiltonian describes two effects seen in electronic excitations of molecular crystals. One, the D-shift due to dispersion, is a displacement in energy between the free molecule and the crystal and is accounted for by the first sum in the equation. The other, described by the second summation, is related to the excitation exchange interaction which is manifested in the factor group or Davydov splitting of the various excitons of differing symmetry.

In order to calculate the exciton energy, the wave vector (k) dependent dipole sums must be calculated. The dipole–dipole interaction dyad can be obtained from the tensor

$$\mathbf{T}_{\alpha\beta}(k) = (v_o/4\pi)\sum_R R^{-3}(1 - 3\hat{R}\hat{R})\exp(ik\cdot R) \quad (2)$$

where v_o is the unit cell volume. The summation includes all nonzero radius vectors

$$R = n\alpha - m\beta \quad (3)$$

between molecules $n\alpha$ and $m\beta$ where α and β refer to molecular orientation and sites within unit cells n and m, respectively. Utilizing the Ewald–Kornfield summation method[20] the dipole sums can be rewritten as

$$\mathbf{T}_{\alpha\beta}(k) = \mathbf{t}_{\alpha\beta}(k) + \hat{k}\hat{k} \quad (4)$$

The $\mathbf{t}_{\alpha\beta}(k)$ term is an analytic function of the wave vector. The $\hat{k}\hat{k}$ term is a macroscopic or long-range term which introduces

(17) Ridley, J.; Zerner, M. *Theor. Chim. Acta.* **1973**, *32*, 115.
(18) Philpott, M. R. *J. Chem. Phys.* **1969**, *50*, 5117.
(19) Philpott, M. R. *Adv. Chem. Phys.* **1973**, *23*, 227.
(20) Born, M.; Huang, K. *Dynamical Theory of Crystal Lattices*; Oxford University Press: Oxford, 1954; p 248.

directional dependence into the lattice sum. It can be calculated by the product.

$$(\hat{d}_{\alpha X}\cdot\hat{k})(\hat{k}\cdot\hat{d}_{\beta Y}) \tag{5}$$

where $\hat{d}_{\alpha X}$ and $\hat{d}_{\beta Y}$ are unit vectors in the direction of the electronic transitions, X and Y, of molecules having orientations α and β, respectively. The exciton energies can be obtained by solving the equation[21]

$$[1\delta_{\alpha\beta}\delta_{XY} + 4\pi\alpha_X \mathbf{T}_{\alpha X,\beta Y}] = 0 \tag{6}$$

where

$$4\pi\alpha_X(\omega) = \sum_{\alpha} \omega_0^2 f_{\alpha X}/(\omega_{\alpha X}^2 - \omega^2) \tag{7}$$

and $\omega_0^2 = 4\pi e^2/mv_0$. The oscillator strength of the transition is $f_{\alpha X}$ and $\omega_{\alpha X}$ is its frequency. As shown in eq 7, the exciton splitting is proportional to the oscillator strength of the transition involved. Finally, the dipole sum in eq 6 is calculated from eq 2 by

$$\mathbf{T}_{\alpha X,\beta Y}(k) = \hat{d}_{\alpha X}\cdot\mathbf{T}_{\alpha\beta}(k)\cdot\hat{d}_{\beta Y} \tag{8}$$

The various branches of the excitons transform according to the irreducible representations of the point group of the unit cell symmetry. The DSP molecular crystal factor group is D_{2h} and thus the four branches of the exciton will be of either A_u, B_{1u}, B_{2u}, or B_{3u} symmetry. The symmetries dictate which branch will be observed in each spectrum.

III. Discussion

A. Absorption Spectra. The 12 K, single crystal, specular reflectance spectra transformed to absorption spectra are shown in Figure 4. It is immediately apparent that these spectra display rather complex electronic structure. The *a*-axis spectrum ([100] direction) appears to have a vibronic progression beginning at 23 000 cm^{-1}. Another band, almost completely obscured by a higher intensity vibronic band, appears at 23 450 cm^{-1}. Finally, the vibrational progression of a higher energy transition is observed to begin at 31 000 cm^{-1}. For the *c*-axis polarization ([001] direction), there is a lower intensity system beginning at 23 250 cm^{-1} followed by a quite intense vibronic progression beginning at 25 200 cm^{-1}. The higher energy band observed in the *a*-axis spectrum is also visible at about 31 500 cm^{-1}. The *b*-axis spectrum ([010] direction) shows very little absorption below 31 000 cm^{-1}. Due to the intensity and apparent factor group splittings of the main transitions in these spectra, the oriented gas model is not applicable.

Consideration of the geometry of the DSP molecule in the unit cell along with symmetry constraints aid in assignment of the observed transitions. Although the crystal packing distorts the molecule, it retains approximate C_{2h} symmetry. Thus the spectroscopically allowed molecular transitions are mainly A_u (*z*-axis polarized) or B_u (polarized in the *xy* plane, see Figure 4). The long axis (*y*-axis) of the molecule is nearly perpendicular to the *b* crystallographic axis and forms a 60° angle with the *a*-axis (see Figure 5). Since there is no observable intensity in the spectrum polarized along the *b*-axis until above 30 000 cm^{-1}, any transitions at lower energy must be polarized along either the long axis of the molecule (*y*-axis) or normal to it (*z*-axis). Thus, the B_u transition in this energy region will be a $\pi^* \leftarrow \pi$ transition polarized along the long axis of the molecule and an A_u will be an $\pi^* \leftarrow$ n transition polarized out of the molecular plane.

Considerable study of the excited states of pyrazine has been reported, and it has been shown that the lowest excited state is a $\pi^* \leftarrow$ n transition.[22,23] This is characteristically the lowest energy transition in azabenzenes.[24] Due to its central pyrazine ring, DSP should have a $\pi^* \leftarrow$ n transition as its lowest excited state, and, typical of these transitions, it is expected to be of low intensity. In spite of this, the $\pi^* \leftarrow$ n transition has been largely ignored in the analysis of the DSP photoreaction. Since this transition is expected to be in the energy region of importance to the photoreaction, its role must be examined.

The properties of the low intensity peaks at approximately 23 350 cm^{-1} in both the *a*- and *c*-axis spectra (Figure 4) suggest that they may be due to an A_u ($\pi^* \leftarrow$ n) transition. Although the spectrum in this region is congested, preventing the accurate determination of polarization ratios, this transition is clearly polarized in a direction different from the more intense transition that almost obscures it. To confirm that this is indeed an $\pi^* \leftarrow$ n transition, DSP was dissolved in a variety of polar and nonpolar solvents, and their spectra were obtained. As is seen in Figure 3, the spectra with polar solvents show the characteristic blue shift of the leading shoulder indicative of the presence of this transition. The INDO/S calculation also supports the existence of the $\pi^* \leftarrow$ n transition as the lowest energy DSP transition. Table II summarizes the experimental and calculational results.

The $\pi^* \leftarrow$ n transition in the crystal spectrum appears to be more intense than predicted by the INDO/S calculation. The apparent discrepancy is due to the distortion in the crystal of the

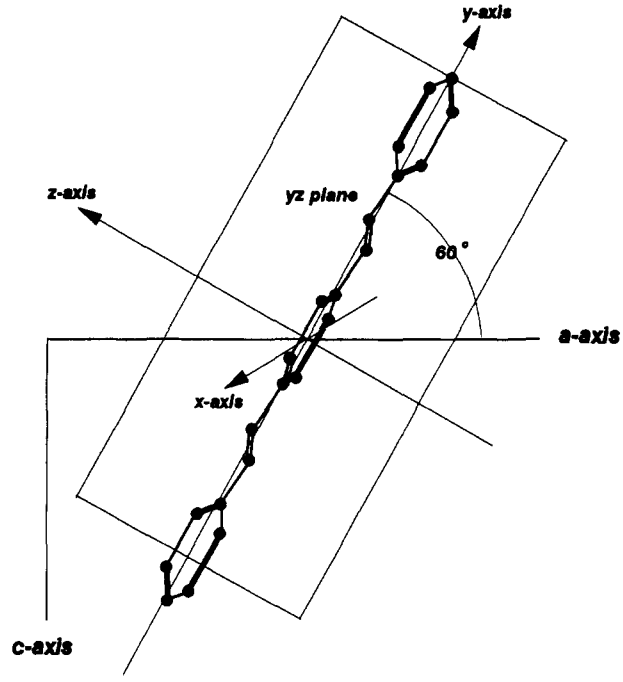

Figure 5. The crystallographic (*a*,*c*) and symmetry axes (*x*,*y*,*z*) of the DSP monomer. *a*, *b*, and *c* refer to crystallographic axes while *x*, *y*, and *z* refer to the coordinate system with respect to the free DSP molecule.

Table II. Calculated and Experimental Values for the Transitions of DSP

calculated				observed[a]			
sym-metry	type	energy (cm^{-1})	oscillator strength	sym-metry	type	energy (cm^{-1})	oscillator strength
^1A_u	$\pi^* \leftarrow$ n	29 564	0.0078	^1A_u	$\pi^* \leftarrow$ n	≈24 200[b]	≈0.026[b]
^1B_u	$\pi^* \leftarrow \pi$	30 101	1.8215	^1B_u	$\pi^* \leftarrow \pi$	24 900	≈2.50
^1A_u	$\pi^* \leftarrow$ n	36 657	0.0006				
^1B_u	$\pi^* \leftarrow \pi$	36 868	0.4223	^1B_u	$\pi^* \leftarrow \pi$	31 700	≈1.28

[a] The experimental values were obtained from the solution spectrum in THF. [b] Although its existence was confirmed, the solution and low-temperature glass (EPA) spectra allowed only estimation of the energy and the oscillator strength of the $\pi^* \leftarrow$ n transition.

(21) Clark, L. B.; Philpott, M. R. *J. Chem. Phys.* **1970**, *53*, 3790.
(22) Innes, K. K.; Simmons, J. D.; Tilford, S. G. *J. Mol. Spectrosc.* **1963**, *11*, 257. Lim, E. C.; Tanin, A. *Spectrosc. Lett.* **1972**, *5*, 35.
(23) El-Sayed, M. A.; Robinson, G. W. *Mol. Phys.* **1961**, *4*, 273.
(24) Innes, K. K.; Byrne, J. P.; Ross, I. G. *J. Mol. Spectrosc.* **1967**, *22*, 125.

Table III. Calculated and Experimental Values of the Exciton Energies of the $\pi^* \leftarrow$ n Transition and the Vibronic Progression of the $\pi^* \leftarrow \pi$ Transition in the (010) Face of the DSP Crystal

	calculated values (cm^{-1})				experimental values (cm^{-1})			
transition	*a*-axis	*c*-axis	splitting	PR[a]	*a*-axis	*c*-axis	splitting	PR[a]
$\pi^* \leftarrow$ n	24 205	24 091	114	9.5	23 500	23 250	250	4.0
0 $\pi^* \leftarrow \pi$	22 333	24 453	2,120	1.2	23 000	25 200	2,200	2.5
1 $\pi^* \leftarrow \pi$	25 284	25 492	208	4.7	24 600	26 250	1,650	1.8
2 $\pi^* \leftarrow \pi$	26 557	26 675	118	3.7	25 900	27 350	1,450	2.6
3 $\pi^* \leftarrow \pi$	27 666	27 750	84	3.4	27 250	28 350	1,100	2.5
4 $\pi^* \leftarrow \pi$	28 763	28 813	50	3.2	28 550	29 300	750	2.3

[a] Polarization (dichroic) ratio *a*-axis/*c*-axis.

molecule from its model planarity. Packing causes the DSP molecule to twist to a dihedral angle of 12.09° between the central pyrazine and the distal phenyl rings.[5] This effectively lowers the symmetry from C_{2h} to C_i allowing intensity borrowing from the $\pi^* \leftarrow \pi$ transition because of the mixing of states induced by the deformation. The presence of the $\pi^* \leftarrow$ n transition in the energy region of the first oligomerization stage of the reaction suggests that it may be of significance to the reaction.

The most prominent transition in DSP is that beginning at 23 000 cm^{-1} in the *a*-axis spectrum and at 25 200 cm^{-1} in the *b*-axis spectrum. The polarization ratio (*c*-axis/*a*-axis) for this transition is 2.76 while the theoretical ratio for a B_u long axis transition is 3. Since this corresponds to a difference of merely 1°, this $\pi^* \leftarrow \pi$ transition is assigned as polarized along the molecular long axis. Furthermore, the INDO/S calculation is in agreement with this assignment. A salient feature of this transition is the large Davydov (factor group) splitting of 2200 cm^{-1} between the *a*- and *c*-axis spectra. In the *c*-axis spectrum, this transition begins at 25 200 cm^{-1} while for that polarized along the α-axis, the origin is at 23 000 cm^{-1}. This large factor group splitting is indicative of significant delocalization of the exciton.

The highest energy transition in these spectra is also rather intense and is located at approximately 31 700 cm^{-1} in all three spectra. The fact that this does have intensity in the *b*-axis spectrum suggests that it is a $\pi^* \leftarrow \pi$ transition polarized along the molecular short axis which is in agreement with the INDO/S calculation. It has a transition dipole strength of 1.16 $Å^2$. Since it is above 30 000 cm^{-1} (333 nm), it is of little importance to the oligomerization photochemical reaction.

B. Excitonic Interactions. Since the facilitating role of excitons in the photoreaction of DSP has been previously suggested,[6,8,11] it is necessary to investigate more thoroughly the effects of excitonic interactions observed in the DSP spectra. The large factor group splitting observed in the polarized absorptivity spectra also indicates that there are significant exciton interactions. To determine the strength of the exciton interaction in DSP, model calculations were performed for the monomer crystal and the results compared to the crystal absorption spectra. The results of these calculations for the (010) face are summarized in Table III. Since the transition dipole strength of the low intensity $\pi^* \leftarrow$ n transition could not be determined unambiguously from the solution spectrum, various calculations were performed using double and half of the dipole strength listed in Table II. This only affected the exciton splitting of this transition slightly and it had negligible effect upon the $\pi^* \leftarrow \pi$ transition splitting.

The calculations show a *D*-shift of 1067 cm^{-1} and an overall exciton splitting of 2120 cm^{-1} between the B_{1u} and the B_{3u} branches of the exciton for the $\pi^* \leftarrow \pi$ transition. The B_{1u} exciton component is polarized along the *c*-axis while the B_{3u} is polarized along the *a*-axis. These results are in reasonable agreement with the experimental values for the *D*-shift and exciton splitting of 900 and 2200 cm^{-1}, respectively. As noted from the spectra, the vibronic progression in the *a*-axis spectrum has a larger vibrational splitting than does the *c*-axis spectrum. The calculations predict an average vibronic progression of 1608 cm^{-1} for the *a*-axis spectrum and 1090 cm^{-1} for the *c*-axis. The experimental values of 1388 ± 70 and 1025 ± 70 cm^{-1}, respectively, quite well mirror the trends shown by the calculations and demonstrate that the difference is merely due to the exciton splitting of the same vibrational progression. In light of the spectral congestion and ensuing difficulty in deconvoluting the vibronic structure for assignment of the Franck–Condon factors, the agreement between the calculated and experimental exciton assignments is quite good.

These calculations and experimental determinations establish that the $\pi^* \leftarrow \pi$ transition in DSP involves sizable Davydov splitting indicating substantial exciton mobility. Since this is the major transition in the energy region of interest to the photochemistry, this delocalized exciton must play an important role in the reacting crystal. The calculations and experiment also demonstrate that the exciton splitting is considerably larger that the *D*-term dispersion for the $\pi^* \leftarrow \pi$ transition.

The $\pi^* \leftarrow$ n transition shows a much smaller exciton splitting as is expected from its low intensity. The branches of this exciton have only a 250 cm^{-1} splitting at most. The *D*-shift, however, is much larger. From the solution spectrum in tetrahydrofuran, the energy of this transition is around 24 200 cm^{-1}, while in the crystal, it is centered at 23,350 cm^{-1}. The shift calculated from this difference is 850 cm^{-1} although this value must be viewed with some caution due to the uncertainty of the transition energy in the solution spectrum. Nevertheless, unlike the $\pi^* \leftarrow \pi$ transition, this transition has a much larger dispersion shift than exciton splitting which is only about a tenth of that seen for the $\pi^* \leftarrow \pi$ exciton. Consequently this excitation is significantly more localized.

C. Exciton–Phonon Interactions. Exciton–phonon coupling occurs when an electronic excitation can perturb the intermolecular potential of the lattice. The promotion of an electron into the excited state alters the local binding energy thus causing a distortion of the lattice and thereby effectively couples the electronic transition and the lattice phonons. The larger the effect of the transition upon the binding energy, the more severe the lattice distortion, expressed as a local strain, will be. Two experimental manifestations of this coupling are line-broadening in the absorption spectrum and the appearance of phonon sidebands.[7] Since it has been suggested that the reactivity of DSP is due to exciton–phonon interactions,[8] it is necessary to investigate the possibility of such coupling in this molecular crystal. The exciton–phonon interaction is an important mechanism for generating lattice strain whose role in solid-state reactions has been recently emphasized and explored theoretically.[25]

To clarify this coupling, the exciton formalism is reexamined. The exciton Hamiltonian of eq 1 can be simplified to[7]

$$\mathcal{H}_{ex} = \sum_s (\Delta\epsilon_s + D_s) B_s^\dagger B_n + \sum_{s \neq u} M_{su} B_m^\dagger B_n \qquad (9)$$

where the ground-state energy for the free molecule has been ignored and M_{su} is the excitation exchange interaction between molecules s and u. The coupling of excitons and phonons depends upon the variance of the spatial and orientational coordinates *R* of the molecules. The adiabatic approximation of the exciton–

(25) Luty, T.; Fouret, R. *J. Chem. Phys.* **1989**, *90*, 5696.

phonon Hamiltonian can then be separated into

$$\mathcal{H}_{ex}(R) = \mathcal{H}_{ex}(R_0) + \mathcal{H}_D(R) + \mathcal{H}_M(R) \qquad (10)$$

where $\mathcal{H}_{ex}(R_0)$ is the rigid lattice Hamiltonian and $\mathcal{H}_D(R)$ and $\mathcal{H}_M(R)$ are the R-dependent terms of the exchange and dispersion interactions, respectively. In the first coupling limit $\mathcal{H}_M(R) \gg \mathcal{H}_D(R)$, the excitation is mainly delocalized and the exciton–phonon coupling is weak since the level shift, of which $\mathcal{H}_D(R)$ is a function, describes the distortion of the lattice around a propagating exciton. In the second limit $\mathcal{H}_D(R) \gg \mathcal{H}_M(R)$, the exciton is highly localized and the lattice deformation is confined to the site of exciton creation.

In the DSP crystal, *two* excitonic transitions are observed in the region of interest to the photochemistry. As discussed above, the intense $\pi^* \leftarrow \pi$ transition not only is found to have a significant exciton splitting but also this splitting is approximately twice the energy of the level shift. This transition is not, therefore, expected to show a substantial exciton–phonon coupling. Furthermore, Hochstrasser and Prasad[8] point out that phonon sidebands and line broadening in the low-temperature crystal electronic spectrum is an indication of strong exciton–phonon coupling. No phonon sidebands have been reported for DSP to date and, although line-broadening in the DSP spectrum has been reported,[9] no extraordinarily broad bands due to this transition were observed in this study. It has also been observed[26] that in aromatic hydrocarbon crystals where the lowest energy transitions are due to π-electrons, the exciton–phonon coupling is weak. Such electronic transitions are not expected to greatly affect the lattice binding energy. Consequently, this transition has no strong exciton–phonon coupling and forms a delocalized exciton.

The second electronic transition of DSP in the energy region affecting the photochemistry is the $\pi^* \leftarrow$ n transition of much lower intensity. El-Sayed and co-workers[14,23] have done considerable work investigating the electronic transitions of both molecular and crystalline pyrazine. They observed that, in the crystal, there is a significant coupling between the nonbonding electrons and the lattice motions. This results from the strong role that the nitrogen lone electron pairs have in the molecular packing. Analogously in DSP, the $\pi^* \leftarrow$ n transition is expected to display a sizable exciton–phonon coupling. And indeed, it does satisfy the limit $\mathcal{H}_D(R) \gg \mathcal{H}_M(R)$ which is a condition for such coupling to be significant since the exciton is quite localized and the dispersion shift is much larger than the exciton splitting. This leads to a significant lattice distortion at the site of the distortion. Further, the INDO/S calculation shows that this transition involves electron density largely from the central pyrazine ring. Like that in the pyrazine crystal, this transition is expected to display strong exciton–phonon coupling. The effect seen by Prasad and co-workers[27] indicating exciton–phonon coupling was most likely due to this transition. Thus, if coupling of the electronic and vibrational motions has a role in the unusual reactivity of DSP, this transition must also be crucial to the photochemistry.

D. Biexcitonic Mechanism of the DSP Reaction. Various attempts have been made to account for the reactivity of DSP, especially as it relates to the much less reactive P2VB. Ebied and Bridge[7] have found excimeric states in the DSP crystal and suggest that these states may be responsible for the reactivity. This, however, cannot resolve the differing reactivities since P2VB displays the same excimeric formation. Clearly, the mechanism which produces the enhanced reactivity of DSP must be absent in the P2VB crystal.

In order to account for the dynamics of the lattice in solid-state reactions, Prasad[28] has proposed the phonon-assistance mechanism. Phonon-assistance arises from phonon–phonon interactions which cause lattice vibrational modes to broaden and shift to lower energy. This shift has been called mode-softening in analogy to phase transition lattice dynamics. As the mode shifts to lower energy, its amplitude of motion increases. In a reactive crystal, these large amplitudes of motion along the reaction coordinate can assist the reaction much as collisions do in the gas phase. That the DSP reaction is phonon dependent is clear, since at very low temperature there is no appreciable product formation even when the crystal is irradiated at length. Furthermore, we have observed the mode-softening associated with phonon-assistance in the DSP crystal.[29] Such phonon–phonon interactions, however, may not fully describe the energetic pathway of the DSP photoreaction. Since the molecular and crystal structures of DSP and P2VB are nearly identical, their lattice potentials and subsequent vibrations should be quite similar. Thus, the motions found in the DSP crystal that aid in product formation should be present in P2VB as well.

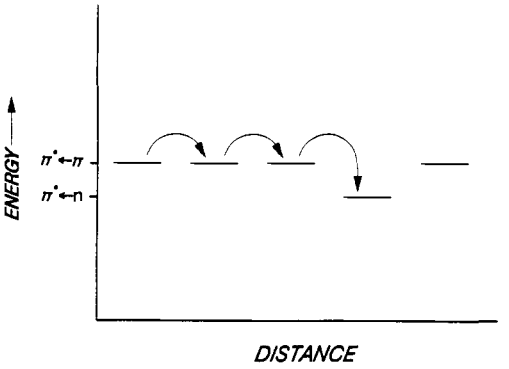

Figure 6. Schematic of the trapping of the delocalized exciton by the lattice distortion created by the exciton–phonon interaction of the $\pi^* \leftarrow$ n transition. The $\pi^* \leftarrow \pi$ designation on the energy scale represents the energy of that delocalized excitation, while the $\pi^* \leftarrow$ n designates the lattice distortion associated with the exciton–phonon interaction which is on the order of kT.

Distinguishing between the photoreactivity of DSP and P2VB requires the investigation of the excitation characteristics of the moieties involved and an understanding of how they couple in the lattice. Clearly, the strong exciton–phonon coupling resulting from the $\pi^* \leftarrow$ n transition of the central pyrazine ring is unique to DSP. This reaction has also been suggested to be biexcitonic, i.e., two separate excitons must interact to initiate product formation.[8] Although the free molecule $\pi^* \leftarrow$ n transition is at lower energy than the $\pi^* \leftarrow \pi$ transition, the exciton splitting in the crystal shifts the B_{3u} component of the $\pi^* \leftarrow \pi$ transition to the region of the lowest energy $\pi^* \leftarrow$ n transition. This places exciton branches of both transitions in the energy region of the first oligomerization reaction, so they both must be involved in the process. The data available from this and past investigations[8,9,23,24] allow formulation of the reaction mechanism where the strong exciton–phonon interaction arising from the $\pi^* \leftarrow$ n transition causes a severe lattice distortion that traps the delocalized exciton of the $\pi^* \leftarrow \pi$ transition to initiate the reaction. This is shown schematically in Figure 6. In this manner, both the delocalized $\pi^* \leftarrow \pi$ exciton and the local exciton–phonon interaction from the $\pi^* \leftarrow$ n transition are integrally involved in the reaction thus causing it to be biexcitonic. This is further supported by the observation that as the temperature is increased above room temperature, the DSP reaction is decelerated.[10] As the temperature is raised, the exciton will not be as readily trapped by the exciton–phonon lattice distortion since it will have sufficient thermal energy to escape. Since the exciton–phonon coupling assistance in DSP results from the $\pi^* \leftarrow$ n transition of the central

(26) El-Sayed, M. A.; Moomaw, W. R. In *Excitons, Magnons and Phonons in Molecular Crystals*; Zahlan, A. B., Ed.; Cambridge University Press: Cambridge, 1968; p 103.
(27) Prasad, P. N.; Swiatkiewicz, J. *Mol. Cryst. Liq. Cryst.* **1983**, *93*, 25.
(28) Prasad, P. N.; Dwarakanath, K. *J. Am. Chem. Soc.* **1980**, *102*, 4254.
(29) Stezowski, J. J.; Peachey, N. M.; Goebel, P.; Eckhardt, C. J. Submitted to *J. Am. Chem. Soc.*

pyrazine ring, the P2VB crystal which has a much different type of $\pi^* \leftarrow$ n transition cannot experience this enhanced reactivity. This mechanism will, of course, only be applicable to reaction of the monomers. The excitonic interactions possible in the monomer will not necessarily be operative in the oligomer, and thus the second stage of this reaction requires more energetic illumination to form the high polymer. This is especially true since the absorption of the oligomers has been shifted to higher energy due to the loss of conjugation.

The local nature of the trap further rationalizes the formation of oligomers instead of high polymers. The lattice distortion and localization of the energy for photoreaction prevent generation of the high polymer but rather favor formation of shorter segments. The existence of a strong exciton–phonon interaction which aids the crystal reactivity does not, however, preclude the possibility of phonon-assistance by phonon–phonon coupling. There is no intrinsic property of these interactions which necessarily excludes the other. And, in fact, the role of phonon–phonon coupling in DSP has been demonstrated.[29] Nevertheless, since the differences of DSP and P2VB are distinguished by the exciton–phonon coupling, this mechanism offers the most satisfactory explanation of their contrasting reactivity. Furthermore, it is not entirely clear whether the observed mode-softening is facilitating the reaction or is merely a consequence of it.

IV. Conclusions

Although organic solid-state reactions have been investigated intensively for several decades, many questions remain unanswered. This may be attributed to the preponderant emphasis placed upon structural considerations. While it is clear that structural viability is a necessary condition for a solid-state reaction, it is certainly not a sufficient one. In order to fully describe solid-state reactivity, a comprehensive approach is required which couples structural studies with dynamic and energetic analyses of the lattice processes.

The DSP solid-state photochemical reaction is a case in point. The unusually high reactivity of the crystal in contrast to that of the isomorphous P2VB crystal has prompted an investigation that delves into aspects beyond structure. The results of this research have established that there are two excitonic states in the DSP molecular crystal in the energy region of the photoreaction rather than only one as previously thought.[9,30] These arise from an intense $\pi^* \leftarrow \pi$ transition polarized along the DSP molecular long axis and a much weaker $\pi^* \leftarrow$ n transition polarized normal to the plane of the pyrazine ring. The intense $\pi^* \leftarrow \pi$ transition in the crystal forms a delocalized exciton as indicated by the large Davydov splittings between its various branches. In contrast, the weaker $\pi^* \leftarrow$ n transition does not lead to appreciable exciton splitting. The *D*-shift resulting from dispersion interactions is much larger than the $\pi^* \leftarrow$ n exciton splitting and thereby leads to a strong local exciton–phonon coupling. Such coupling leads to perturbation of the lattice potential by the lone electron pairs on the central ring nitrogens upon excitation. Since the two crystal excitations occur at essentially the same frequency, they are simultaneously generated and are both crucial to the mechanism of the reaction. The local deformations caused by the $\pi^* \leftarrow$ n exciton–phonon coupling serve as energy traps that initiate the reaction upon the capture of the delocalized $\pi^* \leftarrow \pi$ exciton. The existence of these traps is further supported by the fact that, as the temperature is raised above room temperature, the reactivity decreases.[10]

These results demonstrate the importance of determining the detailed electronic structure of the functional groups comprising the reacting molecule in the crystal. Although the differences between related molecules may be structurally inconsequential, subtle molecular electronic variations can have a profound influence on the collective states of the lattice and, consequently, on the reaction itself. The crystal can act in some sense as an "amplifier" of such variations. The electronic structure of the central pyrazine ring of the DSP molecule heavily influences dynamic and energetic processes in the lattice enhancing DSP solid-state reactivity. The absence of such solid-state interactions in the P2VB crystal arises solely from the differing electronic structure of the central phenyl ring that becomes the major factor contributing to the difference in solid-state reactivity from DSP.

Although the crystal affords an environment in which the reactants are more or less fixed in space, it also supports additional collective interactions, not present in other phases, which can dramatically affect the reaction. These collective properties have often been ignored or not properly accounted for in the analysis of these reactions. Such neglect is unfortunate because consideration of the collective interactions so characteristic of crystals may permit heretofore unexploited approaches for the design and control of solid-state reactions. By investigating the photophysics of one of the archetypical organic crystal-to-crystal reactions and elucidating the nature of the collective excitations driving that reaction, this study has demonstrated the necessity of understanding the energetic as well as the structural aspects of organic solid-state chemistry.

Acknowledgment. N.M.P. gratefully acknowledges the University of Nebraska and the University of Nebraska Foundation for the award of graduate fellowships. Prof. Gordon Gallup graciously provided the INDO/S program used for calculations of spectra in this research.

(30) Williams, J. O.; Janecka-Styrcz, K. *Chem. Phys. Lett.* **1980**, *69*, 83.